Eur. J. Mech. A/Solids 20 (2001) 857–872

S0997-7538(01)01179-2/FLA

Hydrogen induced shear localization of the plastic flow in metals and alloys

P. Sofronis [a,*], Y. Liang [a], N. Aravas [b]

[a] *University of Illinois at Urbana-Champaign, Department of Theoretical and Applied Mechanics, 104 South Wright Street, Urbana, IL 61801, USA*
[b] *University of Thessaly, Department of Mechanical and Industrial Engineering, Pedion Areos, 38334 Volos, Greece*

(Received 19 March 2001; revised and accepted 3 September 2001)

Abstract – Hydrogen enhanced localized plasticity (HELP) is a viable mechanism for hydrogen embrittlement supported by experimental observations. According to the HELP mechanism, hydrogen induced premature failures result from hydrogen induced plastic instability which leads to hydrogen assisted localized ductile processes. The objective of this work is to reveal the role of hydrogen in possibly localizing the macroscopic deformation into bands of intense shear using solid mechanics methodology. The hydrogen effect on material deformation is modeled through the hydrogen induced volume dilatation and the reduction in the local flow stress upon hydrogen dissolution into the lattice. Hydrogen in assumed to reside in both normal interstitial lattice sites (NILS) and reversible traps associated with the plastic deformation. The analysis of the plastic deformation and the conditions for plastic flow localization are carried out in plane strain uniaxial tension. For a given initial hydrogen concentration in the unstressed specimen, a critical macroscopic strain is identified at which shear localization commences. © 2001 Éditions scientifiques et médicales Elsevier SAS

hydrogen / embrittlement / plasticity / localization

1. Introduction

Hydrogen embrittlement, or hydrogen-induced fracture, is a severe environmental type of failure (Birnbaum, 1979, 1983, 1984, 1994; Birnbaum and Sofronis, 1994; Birnbaum et al., 1997; Hirth, 1980, 1984; Johnson, 1984). When hydrogen is present, materials fail at load levels that are very low compared with those that a hydrogen-free material can sustain. Of the many suggestions for an explanation of the hydrogen related failures, the mechanism of hydrogen enhanced localized plasticity (HELP) appears to be a viable one (Beachem, 1972; Meyers et al., 1992; Sirois et al., 1992; Birnbaum, 1988, 1994; Shih et al., 1988; Birnbaum and Sofronis, 1994). Arguments in support of the HELP mechanism are based on experimental observations (Sirois et al., 1992 and Sirois and Birnbaum, 1992) and theoretical calculations (Sofronis and Birnbaum, 1995 and Sofronis, 1995) that in a range of temperatures and strain rates, the presence of hydrogen in solid solution decreases the barriers to dislocation motion, thereby increasing the amount of deformation that occurs in a localized region adjacent to the fracture surface (Tabata and Birnbaum, 1983, 1984; Robertson and Birnbaum, 1986; Bond et al., 1987, 1988; Rozenak et al., 1990; Eastman et al., 1981). The fracture process is a highly localized ductile rupture process rather than an embrittlement (Lee et al., 1977, 1979-a, 1979-b and Onyewenyi and Hirth, 1983). This counterintuitive argument says that the macroscopic ductility is limited by the onset of extensive localized plasticity and is supported by microscopic observations. High-resolution fractography of hydrogen embrittled metals, such as Ni and Fe, show extensive plastic deformation localized along the fracture surfaces (Eastman et al., 1981 and Matsumoto et al., 1981). The technique of in-situ environmental cell deformation and fracture

* Correspondence and reprints.
E-mail address: sofronis@uiuc.edu (P. Sofronis).

carried out for bcc, fcc, and hcp metals having various solute contents, precipitation strengthened alloys, and intermetallics (Tabata and Birnbaum, 1983, 1984; Robertson and Birnbaum, 1984, 1986; Bond et al., 1987, 1988; Rozenak et al., 1990; Xiao, 1993) demonstrates the same localized plasticity character of hydrogen embrittlement despite some differing details among the various cases.

The underlying principle in the HELP mechanism is the shielding of the elastic interactions between dislocations and obstacles by the hydrogen solutes (Sirois and Birnbaum, 1992; Birnbaum and Sofronis, 1994; Sofronis and Birnbaum, 1995; Sofronis, 1995). Reduction of the interaction energies between elastic stress centers results in enhanced dislocation mobility. This phenomenon is supported by strong experimental evidence and has been observed in fcc (Robertson and Birnbaum, 1986), bbc (Tabata and Birnbaum, 1984), and hcp (Shih et al., 1988) systems and in relatively pure materials, in solid solutions alloys, in precipitation strengthened alloys (Bond et al., 1987), and in γ' strengthened alloys (Robertson and Birnbaum (unpublished work on gamma prime strengthened alloys, 1987); Robertson et al., 1984). As a consequence, the intrinsic material flow stress varies with position in an inhomogeneous distribution of hydrogen and is lower where the hydrogen concentration is greater.

The critical question though that still remains unanswered is how this hydrogen induced material softening at the microscale can cause shear localization at the macroscale. As Birnbaum et al. (1997) discuss, it is clear that the flow stress in the region of localization is reduced relative to the flow stress in the homogeneously deforming volume, but the mechanism by which hydrogen causes shear localization has not been established as of yet.

The purpose of this work is to provide a theoretical explanation for the onset of the shear localization in the presence of hydrogen from a solid mechanics point of view. First, the amount of hydrogen in the specimen is calculated by considering the extent of plastic straining (trapped hydrogen) and hydrostatic stress (normal interstitial interstitial hydrogen). In view of the very high mobility of the hydrogen solute, hydrogen concentration in trapping sites is assumed always to be in equilibrium with hydrogen in interstitial sites, which is also assumed to be in equilibrium with local hydrostatic stress. The calculated hydrogen concentration is then used to estimate the amount of material softening along the lines of the experimental observations by Tabata and Birnbaum (1983). The underlying idea is that by accounting for the hydrogen effect on the material constitutive law one can predict the onset of plastic instability in a homogeneously deforming specimen stressed in uniaxial tension. The criterion for the inception of such deformation instability is based on the analytical framework established by the work of Rice (1976) and Rudnicki and Rice (1975).

It should be pointed out that the numerical predictions of shear localization in our chosen model system, e.g. niobium, turn out to be independent of the amount of trapped hydrogen. However, this result is an exception rather than the rule and only a consequence of the trapping model assumed, as discussed in Section 6. To preserve the generality of the present model, as it could apply to other systems with different trapping mechanisms and characteristics, the trapping effect is included in the analysis.

2. Equilibrium hydrogen populations in normal interstitial lattice sites (NILS) and trapping sites

Hydrogen is assumed to reside either at normal interstitial lattice sites or reversible trapping sites at microstructural defects generated by plastic deformation. The two populations are always in equilibrium according to Oriani's theory (1970), such that:

$$\frac{\theta_T}{1-\theta_T} = \frac{\theta_L}{1-\theta_L} K_T, \tag{1}$$

where θ_L denotes the occupancy of the interstitial sites, θ_T denotes the occupancy of the trapping sites,

$$K_T = \exp(W_B/RT) \tag{2}$$

represents the equilibrium constant, W_B is the trap binding energy, R is the gas constant equal to 8.31 J mole^{-1} K^{-1} and T is the absolute temperature. The hydrogen concentration C_T, measured in atoms per unit volume, in trapping sites can be phrased as:

$$C_T = \theta_T \alpha N_T, \tag{3}$$

where α denotes the number of sites per trap and N_T denotes the trap density measured in number of traps per unit volume. The hydrogen concentration C_L, measured in hydrogen atoms per unit volume, in interstitial sites can be stated as:

$$C_L = \theta_L \beta N_L, \tag{4}$$

where β denotes the number of NILS per solvent atom and N_L denotes the number of solvent atoms per unit lattice volume given by:

$$N_L = N_A/V_M, \tag{5}$$

where $N_A = 6.0232 \times 10^{23}$ atoms per mole is Avogadro's number and V_M is the molar volume of the host lattice measured in units of volume per lattice mole.

Hydrogen concentrations in the NILS are studied under equilibrium conditions with local Cauchy stress σ_{ij}. The Fermi–Dirac form (Hirth and Carnahan, 1978) is used to calculate the equilibrium hydrogen concentration C_L in terms of the unstressed lattice concentration C_0 (initial NILS concentration in the absence of any stress, measured in hydrogen atoms per unit volume) as:

$$\frac{\theta_L}{1-\theta_L} = \frac{\theta_L^0}{1-\theta_L^0} K_L, \tag{6}$$

where $\theta_L^0 = C_0/\beta N_L$ denotes the initial NILS occupancy,

$$K_L = \exp(\sigma_{kk} V_H/3RT) \tag{7}$$

is the equilibrium constant dominated by the first-order interaction of hydrogen with stress, V_H is the partial molar volume of hydrogen in solution, and the standard summation convention is used over repeated indices throughout. Transient effects of the type calculated by Fuentes-Samaniego et al. (1984) are not accounted for.

If c_L is the hydrogen concentration in NILS denoting hydrogen atoms per solvent atom:

$$c_L = C_L/N_L = \beta\theta_L \tag{8}$$

by equation (4). Then, the relationship between the corresponding measures for the initial NILS concentration in the unstressed lattice is $c_0 = C_0/N_L$. Similarly, introducing a trapping site concentration c_T measured in trapped hydrogen atoms per solvent atom such that:

$$c_T = C_T/N_L = \beta\theta_{TL}, \tag{9}$$

one calculates $\theta_{TL} = \alpha N_T \theta_T/\beta N_L$ by equation (3). In order for the maximum concentration in both NILS and trapping sites not to exceed that for the MH structure, that is, for the metal hydride, the side condition:

$$c = c_T + c_L \leqslant 1 \tag{10}$$

is imposed, where c is the total hydrogen concentration in both NILS and trapping sites and is measured in hydrogen atoms per solvent atom.

In this paper the hydrogen trap sites are associated with dislocations in the deforming metal (Thomas, 1980 and Angelo et al., 1996). Assuming one trap site per atomic plane threaded by a dislocation (Thomas, 1980; Tien et al., 1976; McLellan, 1979), one finds that the trap site density in traps per cubic meter is given by:

$$N_T = \sqrt{2}\,\rho/a, \tag{11}$$

where ρ is the dislocation density and a is the lattice parameter. Lufrano et al. (1998) maintain that this assumption is consistent with the experimental work of Thomas (1980) in which the best fit to the experimental data was obtained with a trapping radius of only 1 to 2 atomic spacings. The dislocation density ρ measured in dislocation line length per cubic meter was considered to vary linearly with logarithmic strain ε^p (Gilman, 1969):

$$\rho = \begin{cases} \rho_0 + \gamma\varepsilon^p & \text{for } \varepsilon^p < 0.5, \\ 10^{16} & \text{for } \varepsilon^p \geqslant 0.5, \end{cases} \tag{12}$$

where $\rho_0 = 10^{10}$ line length/m^3 denotes the dislocation density for the annealed material and $\gamma = 2.0 \times 10^{16}$ line length/m^3.

Combination of equations (1)–(3), (6)–(12) yields the total hydrogen concentration as a function of both the hydrostatic stress and the equivalent plastic strain, that is:

$$c = \beta\left[\theta_L(\sigma_{kk}) + \theta_{TL}(\sigma_{kk}, \varepsilon^p)\right], \tag{13}$$

where

$$\theta_L(\sigma_{kk}) = \theta_L^0 K_L / \left[(1 - \theta_L^0) + \theta_L^0 K_L\right] \tag{14}$$

and

$$\theta_{TL}(\sigma_{kk}, \varepsilon^p) = \frac{\alpha}{\beta}\frac{N_T(\varepsilon^p)}{N_L}\frac{K_T\theta_L(\sigma_{kk})}{1 - \theta_L(\sigma_{kk}) + K_T\theta_L(\sigma_{kk})}. \tag{15}$$

3. Continuum description of the hydrogen induced softening effect

Birnbaum and Sofronis (1994) have argued that at temperatures and strain rates in which hydrogen embrittlement is experimentally observed, hydrogen induces material softening at the microscale by enhancing the dislocation mobility. In a continuum sense, softening can be described through a local flow stress that decreases with increasing hydrogen concentration. It is important to emphasize here that the term 'local flow stress' denotes the intrinsic flow characteristics of a small volume of material in the microscale, most likely in the neighborhood of a stress raiser, where hydrogen has concentrated by deformation. 'Local flow stress' should not be confused with the flow stress measured 'macroscopically,' say, in a tensile test. The reason is that while the intrinsic material flow stress decreases with hydrogen (Meyers et al., 1992), the macroscopically measured flow stress may either decrease (Beachem, 1972; Matsui et al., 1979-a, 1979-b; Moriya et al., 1979; Eastman et al., 1982) or increase with hydrogen (Asano and Otsuka, 1976; Abraham and Altstetter, 1995) depending on the degree of hydrogen induced shear localization and the magnitude of the local softening due to the removal of dislocation barriers (Birnbaum, 1994; Birnbaum and Sofronis, 1994).

Indeed, Birnbaum (1994) and Birnbaum and Sofronis (1994) demonstrated that when softening induced shear localization takes place, the number of moving dislocations within the specimen reduces since the bulk of

the material outside the shear band(s) ceases to deform. As a result, the dislocation velocity increases in order for the macroscopically imposed machine strain rate to be maintained. Since stress is a response function, this increased dislocation velocity results in an increase of the macroscopic stress (macroscopic hardening). On the other hand, in the absence of shear localization, the macroscopic stress decreases because the dislocations throughout the specimen can keep moving with the same velocity at a lower stress due to shielding of their interactions by hydrogen (macroscopic softening). For example, in the case of stainless steels severe slip localization on a limited number of slip planes is accompanied by significant increases in the macroscopic flow stress (Ulmer and Altstetter, 1991; Abraham and Altstetter, 1995). On the other hand, macroscopic flow stress reduction is observed in the aluminum–hydrogen system (Zeides, 1986) because initial hydrogen clusters which act as barriers to dislocation motion are removed (cut through) by hydrogen enhanced dislocation mobility set by the initial deformation.

It is notable that the experimental procedures used to demonstrate hydrogen-induced hardening have been subject to criticism. Near surface damage by the severe concentration gradients on the surface due to hydrogen charging, phase transformations, and stress induced hydrides at dislocation cores have often been suggested to be the true mechanisms in the observed hydrogen induced hardening (Kimura and Birnbaum, 1987; Birnbaum and Sofronis, 1994). A detailed presentation and discussion of experimental studies of hydrogen induced macroscopic hardening and softening can be found in the work by Abraham and Altstetter (1995).

Based on microscopic studies of the effect of hydrogen on dislocation behavior in iron, Tabata and Birnbaum (1983) determined the local flow stress of the material as a decreasing function of the hydrogen pressure in the environmental cell. Such an experimental observation warrants a continuum description of the hydrogen effect on the local flow stress σ_Y in the form of:

$$\sigma_Y = \sigma_0^H \left(1 + \frac{\varepsilon^p}{\varepsilon_0}\right)^{1/n}, \tag{16}$$

where σ_0^H is the initial yield stress in the presence of hydrogen that decreases with increasing hydrogen concentration, ε_0 is the initial yield strain in the absence of hydrogen, ε^p is the logarithmic strain in uniaxial tension, and n is the hardening exponent that is assumed unaffected by hydrogen. Equation (16) suggests that the hydrogen effect on the local continuum flow characteristics is modeled through the initial yield stress, assumed to be given by:

$$\sigma_0^H = \phi(c)\sigma_0, \tag{17}$$

where $\phi(c)$ is a monotonically decreasing function of the local hydrogen concentration c measured in atoms per solvent lattice atom, and σ_0 is the initial yield stress in the absence of hydrogen. It is assumed that local hydrogen concentrations are such that $c \leqslant 1$, which is typical in bcc systems in which the MH (Metal hydride) structure is allowed to be formed. A possible suggestion for $\phi(c)$ is a linear form:

$$\phi(c) = (\xi - 1)c + 1, \tag{18}$$

where $\xi < 1$ is a parameter. Note that if $c = 1$, then $\phi = \xi$ and $\sigma_0^H = \xi\sigma_0$ denote the ratio of the yield stress in the presence of hydrogen, σ_0^H, to that in the absence of hydrogen, σ_0, at the maximum hydrogen concentration of 1.

The proposed model of equations (16)–(18) for the hydrogen induced material softening should be understood not as a precise and exhaustive description of the experimental findings. Rather, the model should be viewed as an attempt to quantify the experimental understanding of the hydrogen effect on dislocation mobility in a continuum sense. By requiring that ξ is finite and positive, the model does not allow for the

material yield stress to vanish as the hydrogen content c approaches unity. This is indeed an expected realistic feature of the model if one considers that dislocation motion has not been observed to increase indefinitely with hydrogen. In fact, in the present investigation and for low or moderate initial concentrations, that is, for $c_0 \leqslant 0.3$ H/M (H/M denotes hydrogen atoms per metal atom), the function ϕ never assumes values less than 0.69. Therefore, hydrogen never causes the yield stress to reduce by more than 31% in this concentration range. Since the work hardening exponent in equation (1) is treated as independent of hydrogen, the model does not suggest a hydrogen induced change in the deformation mechanism at the microscale. This is also in accordance to the emerging understanding in recent years (Birnbaum et al., 1997) that hydrogen induces material degradation not by altering the local material deformation mechanism, but rather by intensifying it.

4. Constitutive law and conditions for shear localization

4.1. Elastoplastic constitutive law

The total deformation rate tensor D_{ij} (which equals the symmetric part of the velocity gradient in spatial coordinates) is written as the sum of an elastic part, a part due to the presence of hydrogen, and a plastic part:

$$D_{ij} = D^e_{ij} + D^h_{ij} + D^p_{ij}. \tag{19}$$

The elastic behavior of the material is modeled as hypo-elastic, linear and isotropic:

$$D^e_{ij} = \frac{1}{2G}\overset{\nabla}{\sigma}{}'_{ij} + \frac{1}{9K}\overset{\nabla}{\sigma}{}_{kk}\delta_{ij}, \tag{20}$$

where the superposed ∇ denotes the Jaumann or co-rotational stress rate (which exhibits proper material invariance for rigid spin), $\sigma'_{ij} = \sigma_{ij} - \sigma_{kk}\delta_{ij}/3$ is the deviatoric stress, δ_{ij} is the Kronecker delta, and G and K are the elastic shear and bulk moduli respectively.

The stress-free solid at initial solute concentration c_0 is taken as the reference state for measuring strain due to hydrogen induced lattice distortion. The mechanical effect of the hydrogen solute atoms is purely dilatational (Peisl, 1978) and is phrased in terms of the deformation rate as:

$$D^h_{ij} = \dot{\varepsilon}^h \delta_{ij}, \quad \text{where } \varepsilon^h = \ln\left[1 + \frac{\lambda(c - c_0)}{3}\right], \tag{21}$$

a superposed dot denotes material time differentiation, $\lambda = \Delta v/\Omega$, Δv is the volume change per atom of hydrogen introduced into solution that is directly related to the partial molar volume of hydrogen $V_H = \Delta v N_A$ in solution, and Ω is the mean atomic volume of the host metal atom. In view of the definition of ε^h, the expression for D^h_{ij} can be written as

$$D^h_{ij} = \frac{1}{3}\Lambda(c)\dot{c}\delta_{ij}, \tag{22}$$

where $\Lambda(c) = \lambda/[1 + \lambda(c - c_0)/3]$. Note that for small changes of concentration, $\Lambda(c) \approx \lambda$ and equation (22) reduces to the usual infinitesimal strain rate $\dot{\varepsilon}^h_{ij} = (\dot{c}\Delta v/3\Omega)\delta_{ij}$ (Sofronis, 1995).

The material is assumed to be rate independent, to yield according to the von-Mises criterion, and to harden isotropically under plastic straining. The yield criterion is of the form:

$$f = \sigma_e - \sigma_Y\left(\varepsilon^p, c\right) = 0, \tag{23}$$

where $\sigma_e = (3\sigma'_{ij}\sigma'_{ij}/2)^{1/2}$ is the von-Mises equivalent stress, the equivalent plastic strain ε^p is defined as $\varepsilon^p = \int \sqrt{2D^p_{ij}D^p_{ij}/3}\,\mathrm{d}t$, and the flow stress $\sigma_Y(\varepsilon^p, c)$ is defined by equations (16) and (17). The plastic part of the deformation rate is defined by the so-called 'normality condition':

$$D^p_{ij} = \dot{\varepsilon}^p \frac{\partial f}{\partial \sigma_{ij}} = \dot{\varepsilon}^p \frac{3\sigma'_{ij}}{2\sigma_e}. \tag{24}$$

Using the 'consistency condition'

$$\dot{f} = \frac{\partial f}{\partial \sigma_{ij}}\dot{\sigma}_{ij} + \frac{\partial f}{\partial \varepsilon^p}\dot{\varepsilon}^p + \frac{\partial f}{\partial c}\dot{c} = 0, \tag{25}$$

and taking into account the fact that c is a function of σ_{kk} and ε^p (see equations (13–15)), one concludes that:

$$D^p_{ij} = \frac{1}{\frac{\partial \sigma_Y}{\partial \varepsilon^p} + \frac{\partial \sigma_Y}{\partial c}\frac{\partial c}{\partial \varepsilon^p}} \left(\frac{3\sigma'_{kl}}{2\sigma_e} - \frac{\partial \sigma_Y}{\partial c}\frac{\partial c}{\partial \sigma_{pp}}\delta_{km}\delta_{lm} \right) \frac{3\sigma'_{ij}\overset{\nabla}{\sigma}_{kl}}{2\sigma_e}. \tag{26}$$

Substitution of equations (20), (22), and (26) into equation (19) yields the full description of the material constitutive law as follows:

$$\begin{aligned} 2D'_{ij} &= \frac{\overset{\nabla}{\sigma'_{ij}}}{G} + \frac{1}{\frac{1}{3}\left(\frac{\partial \sigma_Y}{\partial \varepsilon^p} + \frac{\partial \sigma_Y}{\partial c}\frac{\partial c}{\partial \varepsilon^p}\right)} \frac{3\sigma'_{ij}}{\sigma_e} \left(\frac{\sigma'_{kl}\overset{\nabla}{\sigma}_{kl}}{2\sigma_e} - \frac{1}{3}\frac{\partial \sigma_Y}{\partial c}\frac{\partial c}{\partial \sigma_{kk}}\overset{\nabla}{\sigma}_{mm} \right), \\ D_{kk} &= \frac{\overset{\nabla}{\sigma}_{kk}}{3\bar{K}} + \frac{\frac{\partial c}{\partial \varepsilon^p}\Lambda(c)}{\frac{1}{3}\left(\frac{\partial \sigma_Y}{\partial \varepsilon^p} + \frac{\partial \sigma_Y}{\partial c}\frac{\partial c}{\partial \varepsilon^p}\right)} \left(\frac{\sigma'_{kl}\overset{\nabla}{\sigma}_{kl}}{2\sigma_e} - \frac{1}{3}\frac{\partial \sigma_Y}{\partial c}\frac{\partial c}{\partial \sigma_{kk}}\overset{\nabla}{\sigma}_{mm} \right), \end{aligned} \tag{27}$$

where $\bar{K} = K/[1 + 3(\partial c/\partial \sigma_{kk})K\Lambda(c)]$.

Comparing the constitutive equations (27) to equations (10) of Rudnicki and Rice (1975), one finds direct analogy between material behavior in the presence of hydrogen and the behavior of pressure sensitive dilatant materials considered by Rudnicki and Rice. In order for the respective equations to be identical, the parameter correspondence is as follows:

Present work		Rudnicki and Rice (1975)
$\frac{1}{3}\left(\frac{\partial \sigma_Y}{\partial \varepsilon^p} + \frac{\partial \sigma_Y}{\partial c}\frac{\partial c}{\partial \varepsilon^p}\right)$	$\rightarrow$	h
$\frac{\Lambda(c)}{\sqrt{3}}\frac{\partial c}{\partial \varepsilon^p}$	$\rightarrow$	β
$-\sqrt{3}\frac{\partial \sigma_Y}{\partial c}\frac{\partial c}{\partial \sigma_{kk}}$	$\rightarrow$	μ
$\bar{K}$	$\rightarrow$	K

(28)

where the parameters h, β, μ, and K in the work of Rudnicki and Rice denote correspondingly the slope of the effective stress–effective plastic strain curve in shear, the dilatancy factor, the pressure sensitivity of yield, and the material bulk modulus. Clearly, hydrogen affects both the material dilatancy and the sensitivity of yield. In

addition, because $\partial c/\partial \varepsilon^p > 0$ and $\partial \sigma_Y/\partial c < 0$, hydrogen reduces the slope of the equivalent stress–equivalent strain curve, thus favoring localization.

4.2. Conditions for localization

Let $Ox_{\rm I}x_{\rm II}x_{\rm III}$ be a Cartesian coordinate system aligned with the principal stress directions, and $\sigma'_{\rm I} \geqslant \sigma'_{\rm II} \geqslant \sigma'_{\rm III}$ be the principal deviatoric stresses. According to Rudnicki and Rice (1975) and Perrin and Leblond (1993) localization of the plastic flow is possible when the hardening modulus:

$$h = \frac{1}{3}\left(\frac{\partial \sigma_Y}{\partial \varepsilon^p} + \frac{\partial \sigma_Y}{\partial c}\frac{\partial c}{\partial \varepsilon^p}\right) \tag{29}$$

reduces upon loading to the critical value:

$$\begin{aligned}\frac{h_{cr}}{G} = {} & \frac{1+\bar{\nu}}{9(1-\bar{\nu})}(\beta-\mu)^2 - \frac{1+\bar{\nu}}{2}\left(N_{\rm II} + \frac{\beta+\mu}{3}\right)^2 \\ & + \frac{(4-3N_{\rm II}^2)(1+\bar{\nu})}{24\sqrt{3}(1-\bar{\nu})}(\beta-\mu)(\sin 2\theta_0)^2\frac{\sigma_e}{G} + {\rm O}\left(\frac{\sigma_e}{G}\right)^2,\end{aligned} \tag{30}$$

where $\bar{\nu} = (3\bar{K} - 2G)/(6\bar{K} + 2G)$, $\tan\theta_0 = \sqrt{(\xi - N_{\rm III})/(N_{\rm I} - \xi)}$, $N_i = \sqrt{3}\sigma'_i/\sigma_e$, $i = {\rm I, II, III}$, $\xi = [(1+\bar{\nu})(\beta+\mu)/3] - N_{\rm II}(1-\bar{\nu})$, and the loading is such that $N_{\rm III} < \xi < N_{\rm I}$. Rudnicki and Rice also show that the unit normal **n** to the plane of the shear band is perpendicular to the direction $x_{\rm II}$, and that the angle θ between **n** and direction $x_{\rm III}$ is:

$$\theta = \theta_0 + \frac{1}{\sqrt{3}}\left[\frac{1+\bar{\nu}}{6}(\mu-\beta)\cot 2\theta_0 - \frac{1}{4}\left(1 - \frac{3}{4}N_{\rm II}^2\right)^{1/2}\sin 2\theta_0\right] + {\rm O}\left(\frac{\sigma_e}{G}\right)^2. \tag{31}$$

5. Hydrogen-induced shear localization in plane strain uniaxial tension

The conditions for shear localization are studied in the case of a specimen loaded in homogeneous uniaxial tension under plane strain deformation (see *figure 1*). Loading is effected incrementally by applying displacement increments along the x_2-axis. Before the application of the external load, the specimen was assumed to be stress free and at a uniform initial hydrogen concentration c_0. Upon loading, uniform redistribution of the H solutes occurs within the solid so that hydrogen is always under quasi-static 'local equilibrium' conditions with local stress and plastic strain as discussed in Section 2 (cf. equation (13)). Since hydrogen is assumed to be provided by a chemical reservoir, an arrangement corresponding to 'far field concentration' kept constant at c_0, the calculation corresponds to a constant chemical potential for the hydrogen solute. The first increment of the displacement was such that the specimen was brought to yield as determined by equation (17). Subsequently, the loading was continued with the specimen deforming in the elastoplastic regime. Localization of plastic flow is possible when the hardening modulus h, defined by equation (29), reduces upon loading to the critical value h_{cr}, determined by equation (30).

The solution to the problem of plane strain tension was obtained numerically; details of the calculation are reported in the Appendix.

The numerical computations were carried out with regard to the niobium system, as material data are available for this system. The initial trapping site concentration was calculated from equations (1)–(4), with

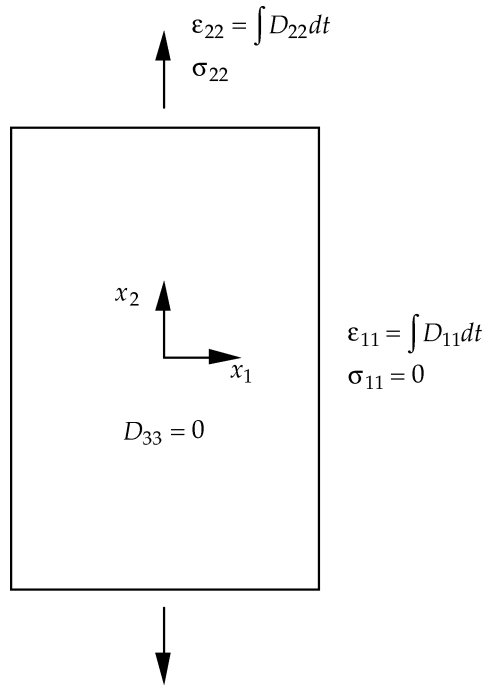

Figure 1. A specimen strained homogeneously in plane strain by displacement increments in the x_2 direction. In the absence of deformation, the specimen is at an initial concentration c_0 measured in hydrogen atoms per solvent atom (H/M).

the parameter α taken to be equal to 1. The parameter β was set equal to 1 and this corresponds to a maximum NILS concentration of 1 hydrogen atom per solvent lattice atom. Hydrogen was assumed to expand the lattice isotropically and its partial molar volume in solution was $V_H = 1.88$ cm^3/mole which corresponds to $\lambda = 0.174$. The molar volume of niobium was 10.852×10^{-6} m^3/mole which implies that the number of the available NILS was $N_L = 5.55 \times 10^{28}$ solvent lattice atoms per m^3. The lattice parameter was $a = 3.3 \times 10^{-10}$ m, the Poisson's ratio $\nu = 0.34$, and Young's modulus $E = 115$ GPa. The trap binding energy was taken to be equal to $W_B = 29.2$ kJ/mole (Baker and Birnbaum, 1972) and the temperature was 300 K.

Figure 2 shows the normalized stress σ_{22}/σ_0 plotted against the equivalent plastic strain during straining up to the localization event for given initial concentrations c_0, material yield stress in the absence of hydrogen $\sigma_0 =$ 400 MPa, and hardening exponent $n = 10$. It is evident that as the initial concentration increases, the material becomes increasingly softer with decreasing tangent modulus, in accordance with the softening behavior described by equations (17) and (18). Notice that while for the hydrogen free material initial yielding is attained at $\sigma_{22}/\sigma_0 = 1.14$, when $c_0 = 0.8$ H/M the corresponding stress is $\sigma_{22}/\sigma_0 = 0.28$. This behavior is strongly dependent on the value of the parameter ξ which defines the reduction of the yield stress at the maximum hydrogen concentration of 1 (see equations (17) and (18)); the value $\xi = 0.1$ is used in the calculations. *Figure 3* shows the normalized concentration c/c_0 plotted against the equivalent plastic strain as a function of c_0. The relative elevation of the concentration c above the initial concentration c_0 reduces with increasing c_0. This is a direct consequence of the softening-induced decrease in the stress triaxiality $\sigma_{kk} = \sigma_{22} + \sigma_{33}$ with increasing initial concentration. *Figure 4* shows the macroscopic normalized true (logarithmic) strain $\varepsilon_{22}/\varepsilon_0$ at localization plotted against the initial hydrogen concentration c_0, for work hardening exponents $n = 5$ and 10 and yield stress $\sigma_0 = 400$ MPa. The macroscopic strain for localization reduces with initial concentration c_0 provided $c_0 \leqslant 0.64$ H/M and $c_0 \leqslant 0.66$ H/M for $n = 5$ and $n = 10$ respectively. On the other hand, for initial concentrations greater than 0.64 H/M and 0.66 H/M respectively for $n = 5$ and $n = 10$, the dependence of

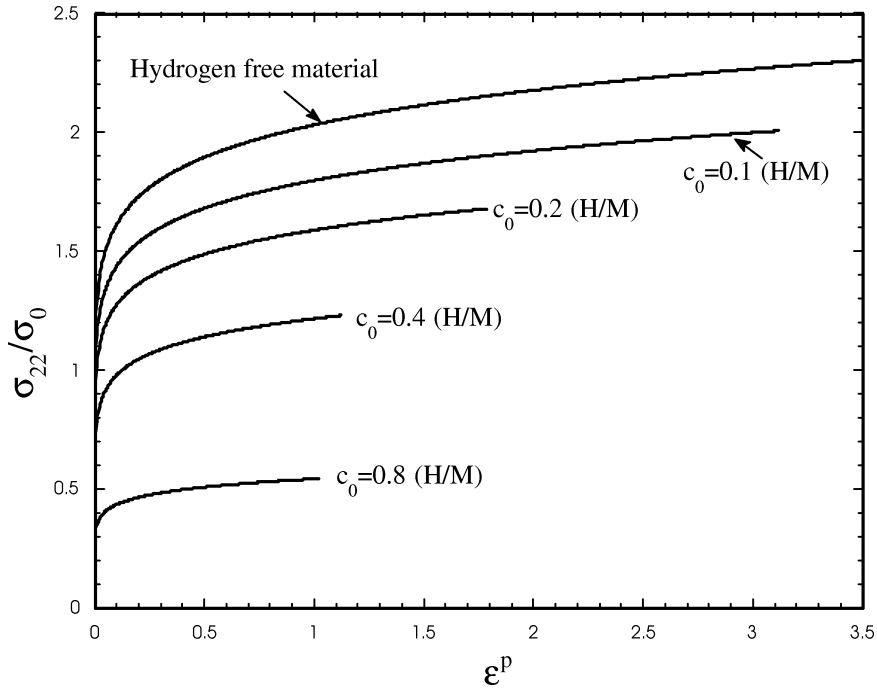

Figure 2. Plot of the normalized stress σ_{22}/σ_0 versus the effective plastic strain ε^p for various initial concentrations c_0. The parameter $\sigma_0 = 400$ MPa is the initial yield stress in the absence of hydrogen. The work hardening exponent was $n = 10$ and the softening parameter ξ was 0.1.

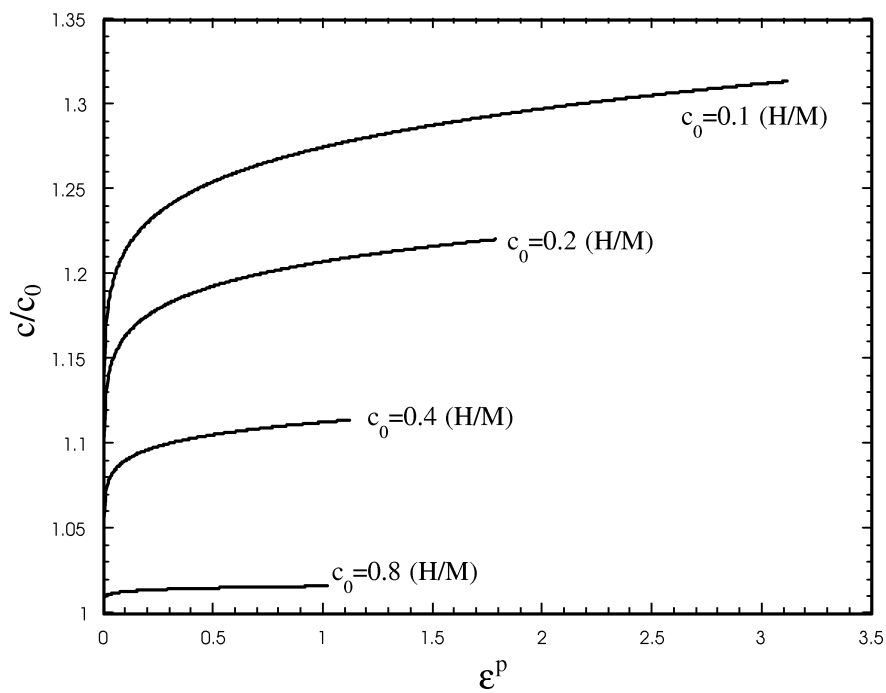

Figure 3. Plot of the normalized hydrogen concentration c/c_0 versus the effective plastic strain ε^p for various initial concentrations c_0. The parameter $\sigma_0 = 400$ MPa is the initial yield stress in the absence of hydrogen. The work hardening exponent was $n = 10$ and the softening parameter ξ was 0.1.

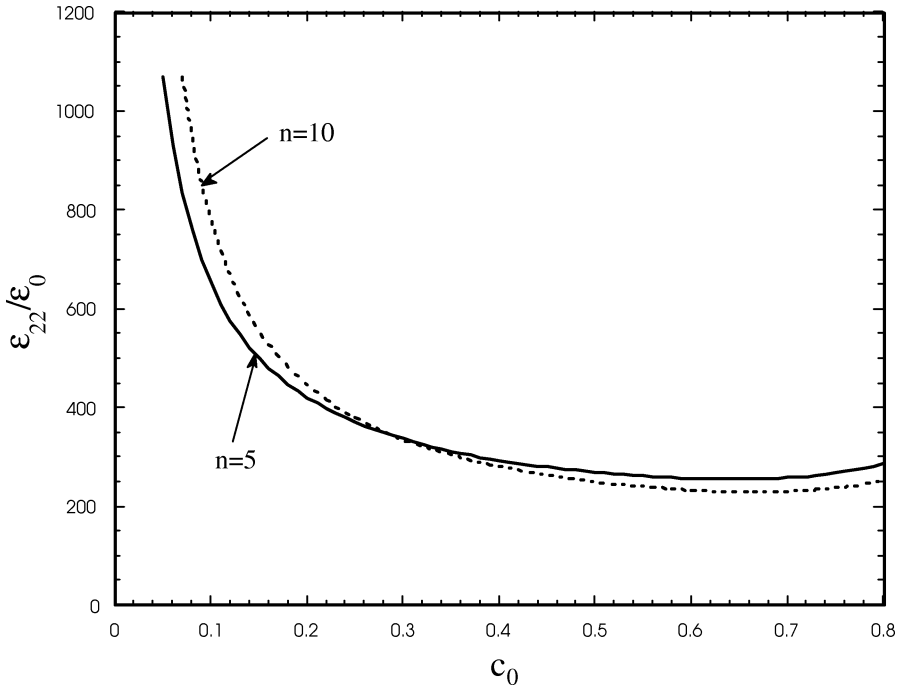

Figure 4. Plot of the normalized macroscopic strain $\varepsilon_{22}/\varepsilon_0$ at localization, bifurcation versus the initial concentrations c_0 for hardening exponents $n = 5,\ 10$. The parameter ε_0 is the initial yield strain corresponding to the yield stress $\sigma_0 = 400$ MPa. The softening parameter ξ was 0.1.

the slope on the initial concentration reverses and the critical strain for localization ε_{22} exhibits only a weak dependence on c_0.

Figure 4 indicates that for initial concentrations c_0 less than 0.29 H/M, the applied strain for localization increases with reducing hardening, i.e. with increasing n. This result is physically plausible because the stress triaxiality necessary to elevate the local concentration c to the levels required for the onset of the localization is achieved at higher strains for the softer material. On the other hand, for initial concentrations greater than 0.29 H/M, the more severe material softening at higher values of n is essentially the factor that governs the condition for localization, and therefore the elevation of triaxiality (i.e. local concentration) required when $n = 10$ is less than that at $n = 5$. This is in accordance with the mild elevations of the hydrogen concentration at high initial concentrations (e.g. $c_0 = 0.8$ H/M) compared to the marked elevations at low initial concentrations (e.g. $c_0 = 0.1$ H/M), as shown in *figure 3*.

6. Discussion

It was demonstrated theoretically that hydrogen can promote localization of the homogeneous macroscopic plastic deformation into bands of intense shear. The model is based on hydrogen induced intrinsic material softening and lattice dilatation both of which have been experimentally verified. The effect of hydrogen is demonstrated in causing the critical modulus for localization to be positive.

The macroscopic strain at which localization takes place depends strongly on the initial hydrogen concentration c_0. At high initial concentrations ($c_0 > 0.3$ H/M), localization has been found in the niobium system (with $n = 10$) to take place at a macroscopic strain of less than $336\varepsilon_0$ and greater than $230\varepsilon_0$. This range corresponds to strains of $80 \div 117\%$. At the initial concentration of $c_0 = 0.3$ H/M, which is moderately

high, localization takes place while the local hydrogen concentration is $c = 0.348$ H/M. At this concentration, the model's prediction is based on the assumption that the local initial yield stress has been reduced to 69% of the yield stress in the absence of hydrogen according to equations (17) and (18). This is not an unrealistic underlying model assumption in view of the experimental evidence on the strong effect of hydrogen on dislocation mobility. Using dislocation velocity measurements, Tabata and Birnbaum (1983) calculated that a reduction of the yield stress by 31% can be achieved at low hydrogen pressures.

Although precise experimental measurements on the strain at localization do not exist, it is generally believed that localization takes place at macroscopic strains, which are close to those just after the material begins to yield. Abraham and Altstetter (1995) observed notable slip localization during tensile tests with 310s stainless steel foils containing as little as 8 at % of hydrogen at macroscopic strain of about 2%. The localization was always accompanied by a negative slope (yield point discontinuity: upper and lower yield point) in the macroscopic stress–strain curve. Of course in an inhomogeneous deformation field, in particular close to stress raisers such as internal defects, grain boundary incompatibilities, and microcracks, the local strain may be many times the initial yield strain ε_0, while the macroscopic strain is just above yield.

Therefore, it can be said that the present model predicts that straining up to fairly high values of macroscopic strain (two orders of magnitude in excess of the material yield strain) is required for the onset of localization in the presence of hydrogen. It is well known that the von Mises flow theory dramatically overestimates the bifurcation strain. Perhaps predictions based on a modified flow model, e.g. one that is based on corner theory, can be one or two orders of magnitude less than those of the present model. However, to adopt such a constitutive model, experimental evidence is required to support that hydrogen can change the flow characteristics of a material in such a way (e.g. yield surface with vertices).

Also the high strains for the onset of localization in the present plane strain study should be viewed in relation to the minimal elevation of the equilibrium hydrogen concentration relatively to the initial concentration. In fact, in the numerical results, equilibrium concentrations c were never larger than the initial concentration c_0 by more than 31%. This is due to the low stress triaxiality attained in plane strain uniaxial tension (*figure 3*) and to the absence of strong hydrogen trapping as discussed below. As a result, both the dilatancy factor ($\sim \partial c/\partial \varepsilon^p$) and the pressure sensitivity of yield ($\sim \partial c/\partial \sigma_{kk}$) were not so dramatically affected (Rudnicki and Rice, 1975) as to allow for shear localization at strains lower than those shown in *figure 4*. It is expected that ahead of a crack tip where the stress triaxiality is higher and the elevation of the hydrogen concentration is much greater (Sofronis and McMeeking, 1989; Taha and Sofronis, 2001), the pressure sensitivity of yield will be higher. It is notable that in the case of high strength steels in which the trapping energy is twice as large as in niobium (Kumnick and Johnson, 1980), the trapped hydrogen concentrations at a crack tip can get as high as 80 times the initial concentration c_0 (Sofronis and McMeeking, 1989; Taha and Sofronis, 2001). Similarly a model of trapping in the form of hydrogen atmospheres around dislocations will also result in higher-pressure sensitivity. Evidently, further studies are required in order to address the sensitivity of the localization condition on the applied macroscopic strain.

In order to quantify the percentage of trapped hydrogen relatively to the total hydrogen in the specimen, one sees that the maximum trap density predicted by equations (11) and (12) is 4.3×10^{25} traps/m^3. Since there are 5.55×10^{28} solvent lattice metal atoms per m^3, one concludes that the trap density is 8×10^{-4} trap sites per solvent metal atom. At this level of trap site density, even with trap saturation, the amount of trapped hydrogen is very small relative to the interstitial hydrogen. As a result, the effect of the trap binding energy on the localization, bifurcation condition is negligible. Parametric studies with defect binding energies equal to 20 and 40 kJ/mole yielded results identical to those shown in *figure 4*.

7. Closure

The present model simulations predict that hydrogen induced localization of plastic deformation in the form of bands of intense shear is indeed a mechanism of deformation possibly occurring at the macroscale. The model is based on realistic material parameters and experimental studies of the hydrogen effect on dislocation mobility. The numerical results seem to overestimate the macroscopic strain required for localization as predicted by experiments. The calculated hydrogen effect can be intensified quantitatively by considering more effective trapping modes of hydrogen in the presence of higher stress triaxialities such as those ahead of a crack tip. The dependence of the hydrogen-induced localization on the nature of the material yield model will be considered in a subsequent publication.

Acknowledgments

This work was supported by the Department of Energy under grant DEFGO2-96ER45439. The authors would like to thank Professors H.K. Birnbaum and C.J. Altstetter for many helpful discussions on the physics of the hydrogen effect on the materials behavior.

Appendix

For the plane strain uniaxial tension problem described in Section 5, the only non-zero stress and deformation rate components are $\sigma_{22}, \sigma_{33}, D_{11} = \dot{\varepsilon}_{11}$, and $D_{22} = \dot{\varepsilon}_{22}$, where ε_{11} and ε_{22} are the logarithmic strains respectively in directions 1 and 2. The corresponding constitutive equations are:

$$\dot{\varepsilon}_{11} = -\frac{\nu}{E}(\dot{\sigma}_{22} + \dot{\sigma}_{33}) + \dot{\varepsilon}^h + \dot{\varepsilon}^p n_{11}, \tag{A1}$$

$$\dot{\varepsilon}_{22} = \frac{1}{E}\dot{\sigma}_{22} - \frac{\nu}{E}\dot{\sigma}_{33} + \dot{\varepsilon}^h + \dot{\varepsilon}^p n_{22}, \tag{A2}$$

$$\dot{\varepsilon}_{33} = -\frac{\nu}{E}\dot{\sigma}_{22} + \frac{1}{E}\dot{\sigma}_{33} + \dot{\varepsilon}^h + \dot{\varepsilon}^p n_{33} = 0, \tag{A3}$$

where

$$n_{ij} = 3\sigma'_{ij}/2\sigma_e. \tag{A4}$$

The yield condition is given by equation (23) as:

$$\sigma_e - \sigma_Y(\varepsilon^p, c) = 0, \tag{A5}$$

and the hydrogen concentration c is given by equation (13) in the form of:

$$c = c(\sigma_{kk}, \varepsilon^p). \tag{A6}$$

Initial yielding

The specimen yields upon loading when the following conditions are satisfied:

$$\varepsilon_{11} = -\frac{\nu}{E}(\sigma_{22} + \sigma_{33}) + \ln\left[1 + \frac{\lambda(c - c_0)}{3}\right], \tag{A7}$$

$$\varepsilon_{22} = \frac{1}{E}\sigma_{22} - \frac{\nu}{E}\sigma_{33} + \ln\left[1 + \frac{\lambda(c - c_0)}{3}\right], \tag{A8}$$

$$0 = -\frac{\nu}{E}\sigma_{22} + \frac{1}{E}\sigma_{33} + \ln\left[1 + \frac{\lambda(c - c_0)}{3}\right], \tag{A9}$$

$$c = c(\sigma_{kk}, 0), \tag{A10}$$

$$\sigma_{22}^2 + \sigma_{33}^2 - \sigma_{22}\sigma_{33} - \sigma_Y^2(0, c) = 0. \tag{A11}$$

The above set of five non-linear equations is solved for $\sigma_{22}, \sigma_{33}, \varepsilon_{11}, \varepsilon_{22}$, and c by using the Newton iteration method.

Plasticity solution

Equations (A1) to (A3) are integrated by using a backward Euler scheme and the solution is determined by the following set of equations:

$$\Delta\varepsilon_{11} = -\frac{\nu}{E}(\Delta\sigma_{22} + \Delta\sigma_{33}) + \frac{1}{3}\Lambda(c_{n+1})\Delta c + \Delta\varepsilon^p(n_{11})_{n+1}, \tag{A12}$$

$$\Delta\varepsilon_{22} = \frac{1}{E}\Delta\sigma_{22} - \frac{\nu}{E}\Delta\sigma_{33} + \frac{1}{3}\Lambda(c_{n+1})\Delta c + \Delta\varepsilon^p(n_{22})_{n+1}, \tag{A13}$$

$$0 = -\frac{\nu}{E}\Delta\sigma_{22} + \frac{1}{E}\Delta\sigma_{33} + \frac{1}{3}\Lambda(c_{n+1})\Delta c + \Delta\varepsilon^p(n_{33})_{n+1}, \tag{A14}$$

$$c_{n+1} = c\big((\sigma_{kk})_{n+1}, \varepsilon_{n+1}^p\big), \tag{A15}$$

$$\big(\sigma_{22}^2\big)_{n+1} + \big(\sigma_{33}^2\big)_{n+1} - (\sigma_{22}\sigma_{33})_{n+1} - \sigma_Y^2\big(\varepsilon_{n+1}^p, c_{n+1}\big) = 0, \tag{A16}$$

where the notation $A_{n+1} = A_n + \Delta A$ denotes the value of A at the end of the increment under consideration. For every increment, the value of $\Delta\varepsilon_{22}$ is prescribed and the quantities $\Delta\varepsilon_{11}, \Delta\sigma_{22}, \Delta\sigma_{33}, \Delta c$, and $\Delta\varepsilon^p$ are determined from the solution of (A12)–(A16) by using the Newton iteration method.

References

Abraham, D.P., Altstetter, C.J., 1995. The effect of hydrogen on the yield and flow stress of an austenitic stainless steel. Met. Trans. A 26, 2849–2858.

Angelo, J.E., Moody, N.R., Baskes, M.I., 1996. Modeling the segregation of hydrogen to lattice defects in nickel, in: Moody, N.R., Thompson, A.W. (Eds.), Hydrogen Effects in Materials. Trans. Met. Soc. AIME, New York, NY, pp. 161–170.

Asano, S., Otsuka, R., 1976. The lattice hardening due to dissolved hydrogen in iron and steel. Scr. Met. 10, 1015–1020.

Baker, C., Birnbaum, H.K., 1972. On the hydrogen-dislocation interaction in niobium. Scr. Met. 6, 851–853.

Beachem, C.D., 1972. A new model for hydrogen-assisted cracking (hydrogen embrittlement). Met. Trans. 3, 437–451.

Birnbaum, H.K., 1979. Hydrogen related failure mechanisms in metals, in: Foroulis, Z.A. (Ed.), Environmental Sensitive Fracture of Engineering Materials, Proceedings of Symposium on Environmental Effects on Fracture, Chicago, Illinois, October 24–26, 1977. Metallurgical Society of AIME, Warendale, PA, pp. 326–360.

Birnbaum, H.K., 1983. Hydrogen related fracture of metals, in: Latanision, R.A., Pickens, J.R. (Eds.), Atomistics of Fracture, Proceedings of a NATO Advanced Research Institute on Atomistics of Fracture, Calcatoggio, Corsica, France, May 22–31, 1981. Plenum Press, New York, pp. 733–765.

Birnbaum, H.K., 1984. Hydrogen related second phase embrittlement of solids, in: Gibala, R., Hehemann, R.F. (Eds.), Hydrogen Embrittlement and Stress Corrosion Cracking, Proceedings of a Troiano Festschrift Symposium, Case Western Reserve University, June 1–3, 1980. ASM, Ohio, pp. 153–177.

Birnbaum, H.K., 1988. Environment-induced cracking of metals, in: Gangloff, R.P., Ive, M.B. (Eds.), Environment-induced Cracking of Metals, First International Conference, Kohler, Wisconsin, 1988. NACE, Houston, TX, pp. 21–29.

Birnbaum, H.K., 1994. Hydrogen effects on deformation-relation between dislocation behavior and the macroscopic stress–strain behavior. Scr. Met. 31, 149–153.

Birnbaum, H.K., Sofronis, P., 1994. Hydrogen-enhanced localized plasticity – a mechanism for hydrogen related fracture. Mater. Sci. & Eng. A 176, 191–202.

Birnbaum, H.K., Robertson, I.M., Sofronis, P., Teter, D., 1997. Mechanisms of hydrogen related fracture – A review, in: Magnin, T. (Ed.), Corrosion Deformation Interactions CDI'96, Second International Conference, Nice, France, 1996. The Institute of Materials, Great Britain, pp. 172–195.

Bond, G.M., Robertson, I.M., Birnbaum, H.K., 1987. The influence of hydrogen on deformation and fracture processes in high-strength aluminum alloys. Acta Metall. 35, 2289–2296.

Bond, G.M., Robertson, I.M., Birnbaum, H.K., 1988. Effects of hydrogen on deformation and fracture processes in high-purity aluminum. Acta Metall. 36, 2193–2197.

Eastman, J., Matsumoto, T., Narita, N., Heubaum, N., Birnbaum, H.K., 1981. Hydrogen effects in nickel embrittlement or enhanced ductility?, in: Bernstein, I.M., Thompson, A.W. (Eds.), Hydrogen in Metals. Metallurgical Society of AIME, New York, pp. 397–409.

Eastman, J., Heubaum, N., Matsumoto, T., Birnbaum, H.K., 1982. The effect of hydrogen on the solid solution strengthening and softening of nickel. Acta Metall. 30, 1579–1586.

Fuentes-Samaniego, R., Gasca-Neri, R., Hirth, J.P., 1984. Solute drag on moving edge dislocations. Phil. Mag. A 49, 31–43.

Hirth, J.P., 1980. Effects of hydrogen on the properties of iron and steel. Met. Trans. A 11, 861–890.

Hirth, J.P., 1984. Theories of hydrogen induced cracking of steels, in: Gibala, R., Hehemann, R.F. (Eds.), Hydrogen Embrittlement and Stress Corrosion Cracking, Proceedings of a Troiano Festschrift Symposium, Case Western Reserve University, June 1–3, 1980. ASM, Ohio, pp. 29–41.

Hirth, J.P., Carnahan, B., 1978. Hydrogen adsorption at dislocations and cracks in Fe. Acta Metall. 26, 1795–1803.

Gilman, J.J., 1969. Micromechanics of Flow in Solids. McGraw-Hill, New York, pp. 185–199.

Johnson, H.H., 1984. Overview of hydrogen degradation phenomena, in: Gibala, R., Hehemann, R.F. (Eds.), Hydrogen Embrittlement and Stress Corrosion Cracking, Proceedings of a Troiano Festschrift Symposium, Case Western Reserve University, June 1–3, 1980. ASM, Ohio, pp. 3–27.

Kimura, A., Birnbaum, H.K., 1987. The effects of cathodically charged hydrogen on the flow stress of nickel and nickel-carbon alloys. Acta Metall. 35, 1077–1088.

Kumnick, A.J., Johnson, H.H., 1980. Deep trapping states for hydrogen in deformed iron. Acta Metall. 28, 33–39.

Lee, T.D., Goldenberg, T., Hirth, J.P., 1977. Hydrogen and plastic instability in deformed, spheroidized 1090 steel, in: Fracture 1977, Vol. 2. University of Waterloo Press, Waterloo, pp. 243–248.

Lee, T.D., Goldenberg, T., Hirth, J.P., 1979-a. Effect of hydrogen on fracture of U-nothced bend specimens of spheroidized AISI 1095 steel. Metall. Trans. A 10, 199–208.

Lee, T.D., Goldenberg, T., Hirth, J.P., 1979-b. Effect of hydrogen on fracture of U-nothced bend specimens of quenched and tempered AISI 4340 steel. Metall. Trans. A 10, 439–448.

Lufrano, J., Sofronis, P., 1998. Enhanced hydrogen concentrations ahead of rounded notches and cracks – competition between plastic strain and hydrostatic stress. Acta Mater. 46, 1519–1526.

Lufrano, J., Symons, D., Sofronis, P., 1998. Hydrogen transport and large strain elastoplasticity near a notch in alloy X-750. Eng. Fracture Mech. 59, 827–845.

Matsui, H., Kimura, H., Moriya, S., 1979-a. The effect of hydrogen on the mechanical properties of high purity iron I. Softening and hardening of high purity iron by hydrogen charging during tensile deformation. Mat. Sci. Engng 40, 207–216.

Matsui, H., Kimura, H., Kimura, A., 1979-b. The effect of hydrogen on the mechanical properties of high purity iron III. The dependence of softening on specimen size and charging current density. Mat. Sci. Engng 40, 227–234.

Matsumoto, T., Eastman, J., Birnbaum, H.K., 1981. Direct observations of enhanced dislocation mobility due to hydrogen. Scr. Met. 15, 1033–1037.

McLellan, R.B., 1979. Thermodynamics of diffusion behavior of interstitial solute atoms in non-perfect solvent crystals. Acta Metall. 27, 1655–1663.

Meyers, S.M. et al., 1992. Hydrogen interactions with defects in crystalline solids. Rev. Mod. Phys. 64, 559–617.

Moriya, S., Matsui, H., Kimura, H., 1979. The effect of hydrogen on the mechanical properties of high purity iron II. Effect of quenched-in hydrogen below room temperature. Mat. Sci. Engng 40, 217–226.

Onyewenyi, O.A., Hirth, J.P., 1983. Effects of hydrogen on Notch ductility and fracture in spheroidized AISI 1090 steel. Metall. Trans. A 14, 259–269.

Oriani, R.A., 1970. The diffusion and trapping of hydrogen in steel. Acta Metall. 18, 147–157.

Peisl, H., 1978. Lattice strains due to hydrogen in metals, in: Alefeld, G., Volkl, J. (Eds.), Hydrogen in Metals I, Topics in Applied Physics, Vol. 28. Springer-Verlag, New York, pp. 53–74.

Perrin, G., Leblond, J.B., 1993. Rudnicki and Rice's analysis of strain localization revisited. J. Appl. Mech. 60, 842–846.

Rice, J.R., 1976. The localization of plastic deformation, in: Koiter, W.T. (Ed.), Proc. of the 14th Int. Congress on Theoretical and Applied Mechanics, Delft. North-Holland, pp. 207–220.

Robertson, I.M., Birnbaum, H.K., 1984. Effect of hydrogen on the dislocation structure of deformed nickel. Scr. Met. 18, 269–274.

Robertson, I.M., Birnbaum, H.K., 1986. An HVEM study of hydrogen effects on the deformation and fracture of nickel. Acta Metall. 34, 353–366.

Robertson, I.M., Tabata, T., Wei, W., Heubaum, F., Birnbaum, H.K., 1984. Hydrogen embrittlement and grain boundary fracture. Scr. Met. 18, 841–846.

Rozenak, P., Robertson, I.M., Birnbaum, H.K., 1990. HEVM studies of the effects of hydrogen on the deformation and fracture of AISI type 316 austenitic stainless steel. Acta Metall. 38, 2031–2040.

Rudnicki, J.W., Rice, J.R., 1975. Conditions for the localization of deformation in pressure-sensitive dilatant materials. J. Mech. Phys. Solids 23, 371–394.

Shih, D., Robertson, I.M., Birnbaum, H.K., 1988. Hydrogen embrittlement of α titanium: in situ TEM studies. Acta Metall. 36, 111–124.

Sirois, E., Birnbaum, H.K., 1992. Effects of hydrogen and carbon on thermally activated deformation in nickel. Acta Metall. 40, 1377–1385.

Sirois, E., Sofronis, P., Birnbaum, H.K., 1992. Effects of hydrogen and carbon on thermally activated deformation in nickel, in: Bruemmer, S.M., Meletis, E.I., Jones, R.H., Gerberich, W.W., Ford, F.P., Staehle, R.W. (Eds.), Parkins Symposium on Fundamental Aspects of Stress Corrosion Cracking. The Minerals, Metals & Materials Society, pp. 173–190.

Sofronis, P., 1995. The influence of mobility of dissolved hydrogen on the elastic response of a metal. J. Mech. Phys. Solids 43, 1385–1407.

Sofronis, P., Birnbaum, H.K., 1995. Mechanics of the hydrogen-dislocation-impurity interactions – I. Increasing shear modulus. J. Mech. Phys. Solids 43, 49–90.

Sofronis, P., McMeeking, R.M., 1989. Numerical analysis of hydrogen transport near a crack tip. J. Mech. Phys. Solids 37, 317–350.

Tabata, T., Birnbaum, H.K., 1983. Direct observations of the effect of hydrogen on the behavior of dislocations in iron. Scr. Met. 17, 947–950.

Tabata, T., Birnbaum, H.K., 1984. Direct observations of hydrogen enhanced crack propagation in iron. Scr. Met. 18, 231–236.

Taha, A., Sofronis, P., 2001. A micromechanics approach to the study of hydrogen transport and embrittlement. Eng. Fracture Mech. 68, 803–837.

Thomas, G.J., 1980. Hydrogen trapping in FCC metals, in: Thompson, A.W., Bernstein, I.M. (Eds.), Hydrogen Effects in Metals. Trans. Met. Soc. AIME, New York, pp. 77–85.

Tien, J.K., Thompson, A.W., Bernstein, I.M., Richards, R.J., 1976. Hydrogen transport by dislocations. Metall. Trans. A 7, 821–829.

Xiao, H.Z., 1993. Effects of hydrogen and stress on the microstructure and microchemistry of Ti_3Al-based intermetallic compounds. PhD thesis, University of Illinois at Urbana-Champaign, Urbana, IL.

Ulmer, D.G., Altstetter, C.J., 1991. Hydrogen-induced strain localization and failure of austenitic stainless steels at high hydrogen concentrations. Acta Metall. 39, 1237–1248.

Zeides, F., 1986. Effect of hydrogen on the mechanical properties and fracture behavior of high purity aluminum. PhD thesis, University of Illinois at Urbana-Champaign, Urbana, IL.